B-6.4.3 On the development of global carbon cycle model

Contact person: Shoichi Taguchi
Senior Researcher
Inter-spheric Environmental Section
Environmental Assessment Department
National Institute for Resources and Environment
Agency of Industrial Science and Technology
Ministry of International Trade and Industry
16-3, Onogawa Tsukuba, Ibaraki, 305-8569, Japan
Tel;+81-298-58-8484, Fax;+81-298-58-8358
E-mail; taguchi@nire.go.jp

Total Budget for FY1996-FY1998 11,228,000 Yen (FY1998, 3,191,000 Yen)

Abstract Seasonal variations of CO_2 emissions from the land biota and oceans are retrieved by use of an inverse method. Concentrations of CO_2, computed by an atmospheric chemical transport model (NIRE-CTM-93), are fitted to the observed CO_2 concentrations in terms of annual mean concentrations between 1984 to 1985, one-year period components, half-year components, and a global trend averaged over the years 1979 to 1996. The emissions due to fossil fuel combustion, those from land biota consisting of thirteen land areas, and those from the ocean consisting of twelve oceanic areas, are considered. The problem is solved by a least squares method, using singular value decomposition. A prior estimate of the emissions due to fossil fuel combustion is used as a tight constraint. When the annual mean emission, the net flux from the land biota during the growing season, and the net flux from the ocean are loosely constrained to zero, the solution indicates that areas consist of two groups. That is, those areas with relatively reliable estimates and those without. No reliable estimates are obtained for Africa, tropical and South America, tropical Asia, the tropical and the South Atlantic Ocean, and the western tropical Pacific. A reasonable global budget is not obtained due to unreliable estimates. The amplitude of the seasonal variations over middle-latitude North America is found to be less than that of some tropical land areas.

Key Words Chemical transport model, Inverse Method, Carbon cycle

1.Introduction

Significant seasonal variations in concentrations of atmospheric CO_2 have been noted since the commencement of systematic measurements, as was demonstrated by *Bolin and Keeling* [1]. They attempted to relate the latitudinal distribution of CO_2 sources and sinks to the latitudinal distribution of concentrations, using a one-dimensional diffusion model. The latitudinal distributions of minor constituents are the result of atmospheric transport, as well as the horizontal distribution of the emissions. The tropical interhemispheric exchange process and vertical transport over the source area are major factors that determine the latitudinal distributions of minor constituents, if the lifetimes of the constituents are longer than a few years. A wide range of latitude distributions has been obtained from transport model intercomparisons (TransCom) [18, 3].

2.Research Objective

When constituents are absorbed and released as the seasons progress, such as in the case of carbon dioxide, a rectification process plays a significant role in the distribution of surface concentrations. Rectification is a term from electrical engineering for a process that results in direct currents from alternating currents. In the context of global carbon cycle studies, the term *rectifier* is used for the annual mean concentration in GCTM that is produced from the horizontal distribution of sources and sinks, which are in balance at each geographical location. Since the interhemispheric exchange of air is governed by the Hadley cell in the tropics, seasonal variations of the strength of the Hadley cell over the tropics, and vertical profiles of CO_2 are potential sources of rectifications [16, 10]. Seasonal variations of the planetary boundary layer (PBL) which modify vertical diffusion, can also potentially produce rectifications when the variations are correlated with the seasonal variations of the emissions [4]. Seasonal variations of local wind directions, if correlated with the seasonal variations of the emissions, also have the potential to produce a rectification [20]. A large range of rectifier strength has been reported by [18], as a result of the TransCom study. In the TransCom study, source and sink distributions were provided by *Fung et al.* [8] who estimated the seasonal variations of CO_2 exchange between the land ecosystem and atmosphere, based on a normalized vegetation index (NDVI), derived from satellite observations and a simple soil model. All GCTMs in the study produced amplitudes of seasonal variations larger than those observed.

Either or both the GCTMs and biospheric models for producing sources and sinks may be responsible for the failure to reproduce the observed seasonal concentrations. The present paper demonstrates the seasonal variations of the CO_2 exchange over land and ocean assuming the GCTM used is correct. A steady state of the seasonal cycle is also assumed. The method may be described as a synthesis inversion, as developed by [5, 6].

3.Research Method

Here, for the sake of convenience, a portion of the theory discussed in *Enting et al.* [5] is replicated. The synthesis inversion seeks to estimate the strength x_μ of the N source/sink processes, by comparing M observed concentrations y_j° (with standard deviations u_j) to responses calculated using an atmospheric transport model. If the model response for observation j to a source μ of unit strength is $H_{j\mu}$, then a fit is made on the assumption that

$$y_j^\circ = \sum H_{j\mu} x_\mu + \epsilon_j \quad , \tag{1}$$

where ϵ_j is observational noise. In the Bayesian formalism, the fit is constrained to take into account prior estimates s_μ of the source strengths.

The synthesis inversion process requires three components:
(i) a prior estimate of the strength of the source elements s_μ, with a specified range p_μ ,
(ii) observational data y_j° with specified uncertainties u_j,
(iii) a global chemical transport model to calculate the responses $H_{j\mu}$.
While the code to obtain solutions is exactly the same, the transport model, source components and dataset differ from those in [5].

A single source element has a fixed horizontal distribution within an area, and temporal variations. The horizontal distribution of emissions due to fossil fuel combustion [11] is fixed in time in the present experiment. Area separations are shown in Fig.1 in which thirteen land area and twelve oceanic area are indicated by the shades. Five temporal variations consisting of a constant emission, the sine and cosine of the annual cycle, and the sine and cosine of the semi-annual cycle are considered over land. Since very little is known about the seasonal cycle of the exchange over the ocean, only the first harmonic

of the year is considered over ocean areas. Based on some preliminary experiments, prior estimates and their uncertainties are specified as follows. Fossil fuel 5.3±0.3 GtC/yr, constant emissions over all land and oceanic area 0.0±2.0 GtC/yr, seasonal component over six land areas (the Amazon, North Africa, tropical Africa, Indonesia, South Africa, and South America) 0.0±0.5 GtC/yr, that over remaining land area 0.0±10.0 GtC/yr, seasonal component over the oceans 0.0±0.5 GtC/yr.

Daily surface monitoring data, biweekly flask samples, and aircraft measurements obtained during the observation period were used for the retrieval. Vertical profiles of concentrations are included, because these data were found to have significant impact on the seasonal cycle of the global burden according to a preliminary study. Flask sampling data from the National Oceanic and Atmospheric Administration/ Climate Monitoring and Diagnostics Laboratory (NOAA/ CMDL) [2] designated as 'complete', were obtained via the internet (ftp.cmdl.noaa.gov). Daily sampling data from the Hungarian Meteorological service and Umweltbundesamt were provided on a CD-ROM, compiled at WDCGG/WMO [22]. Aircraft observations at Cape Grim [15, 14] were also obtained via the internet (atmos.dar.csiro.au). Aircraft sampling data over Japan [21], along a trajectory between Japan and Australia [13] and vertical profiles over Siberia, were provided by Prof. Nakazawa of the University of Tohoku (personal communication).

The uncertainties (1 s.d) are set as 0.1 ppmyr^{-1} for the global trend of 1.41 ppmyr^{-1} (equivalent to 3 GtCyr^{-1} emission) at the South Pole, and 0.3 ppm for the mean concentrations at all other relevant sites. Root mean squares of the residuals of the data from a fitted curve are used for the uncertainties of the annual and semi-annual components (see Table 2).

The model (NIRE-CTM-93) uses a semi-Lagrangian scheme over a horizontal grid having a resolution of 2.5 degrees, and 15 vertical sigma levels (0.99, .925, .85, .7, .5, .4, .3, .25, .2, .15, .1, .07, .05, .03, .01). The CTM is driven by the departure points and planetary boundary layer height dataset, derived from the operationally assimilated meteorological data of the European Center for Medium Range Weather Forecasts (ECMWF) for the year 1992. Concentrations are obtained every 6 hours. Further details are given in *Taguchi* [20]. The integration to create the responses $H_{j\mu}$ starts from a globally homogeneous distribution of 350 ppm and continues for three years, making use of the 1992 meteorological data. The responses $H_{j\mu}$ are calculated at the surface and upper levels of the gridpoints corresponding to observational sites.

4.Result

Mean flux obtained by the inverse problem is demonstrated in Fig.1. Closed circle and open circle correspond to zero flux over land and ocean, respectively. Distances between horizontal bar and the center of circle indicate the mean flux at that area. Uncertainties are shown as length of arrows.

The remarkable feature in Fig.1 is the large uncertainties over Africa and tropical regions. One may note that three oceanic areas (the western equatorial Pacific, equatorial Atlantic, and the South Atlantic) have large (more than 3 GtCyr^{-1} peak to peak) uncertainties, which indicate that the solutions in these areas are unreliable.

The values of the mean emission over Siberia and far North America in Fig.1 are significantly large. The values of the mean flux for these two areas have very small uncertainty, which suggests that the results are valid. In fact, those features are unaltered with the change in constraints, the change in meteorological data for the CTM (experiment using ECMWF/1991), and changes in datasets (experimnets without data at NWR or SUn).

To explain these results by differences in climate, ecosystem, and industry between these areas is beyond the scope of the present study.

The total net flux is unrealistic for all cases, because the ocean areas do not absorb CO_2, which does not agree with previous studies. It is worth considering why the net oceanic flux acts as an emission by looking at Fig.1. First, it should be noted that the inversion system presently used requires huge emissions in tropical regions, both for land and ocean. When examining ocean areas, large emissions are found for the west Equatorial Pacific and Equatorial Atlantic, where the uncertainties are the largest among the twelve oceanic areas in all cases. While no solution exhibits absorption at the highest northern latitudes where deep oceanic water is produced, uncertainties in the solution suggest that the tropical region, rather than high latitude areas, as the source of the error. The global net oceanic flux is expected to become an absorption if the emissions in tropical land areas are increased by additional observational evidence.

The seasonal cycles over land areas in the solution and the estimates by *Fung et al.* [8] are shown in Fig.2. The phases of the seasonal emissions exhibit a marked shift in only three areas. In the area of far North America, the mid summer period reveals emissions in the solution, in contrast to absorption found in the NDVI based estimate. Over northern Africa, both the spring and autumn results are contrary to those found in *Fung et al.* [8]. Over South America, the spring emissions and winter absorption are conspicuous. As was found over the ocean, the seasonal cycle in areas where the amplitude of the cycle is weak may be sensitive to small changes in areas where the seasonal cycle is strong. For other areas, the phase of the seasonal cycle resembles those obtained by *Fung et al.* [8], while the timing of the maximum absorption shifts by one to two months, such as those seen over Europe and China.

The amplitude of seasonal cycle over the middle latitudes of North America in Fig.2 is much less than that found over Indonesia, whose expanse is one third of the area of middle North America. It is suspected that the use of the Siberian site creates a large value of GSNF over Siberia, which may suppress the seasonal cycle over middle North America. It is also speculated that the use of the Niwot Ridge (NWR) results in a small seasonal cycle over North America. To examine these hypotheses, two extra inverse calculations in which the Niwot Ridge data, or all vertical profiles over Surget are excluded, are conducted, There is, however, little impact over the Siberian and middle North American areas.

5.Discussion

The major result of this study was that the global budget of CO_2 was obtained with seasonal components consistent with those observed. In former studies [5, 7], seasonal variations of sources and sinks were prescribed by biospheric models. In those studies, rectifiers produced by the seasonal variations of sources and sinks were determined by the biospheric models, even if the seasonal variations were not consistent with the observations. In the present study, seasonal components were treated as unknown variables and were found to be consistent with observations.

The scheme of area separation used in the present study is temporary and subject to future optimization. There are areas where solving the flux will obviously be difficult, such as the western tropical Pacific and Indonesia. Indonesia is geographically included within the western tropical Pacific (Fig.1). It may be difficult to distinguish this area from the fluctuations of concentrations at a distant region. In the tropics, areas cover both hemispheres, and therefore may be a source of error. The tropical rain forest, which

does not have a seasonal cycle, may be confined to a very narrow region over the equator. The rain data, such as ISLSCP [19], show a clear seasonal migration of the rain bands over tropical Africa, as well as the Amazon. Unfortunately, the monitoring network does not well represent these areas, and no great improvement in the solution can be expected by modifying of the area separation in the region.

The uncertainties obtained in the tropical and Southern Hemisphere land areas demonstrate the importance of the coverage of monitoring sites. Without reductions in the uncertainties at unreliable areas, the global net flux can not be improved. Observed concentrations and flux measurements, or ecological field studies, especially in savanna regions, the tropics, and Southern Hemisphere, may help to reduce the uncertainties. The current progress in the standard gas intercomparison project conducted by the WMO (personal communication Prof. Nakazawa) has the potential to increase available data. Other improvements are expected by the application of the Global View dataset [12]. Improvements in the results of the inverse calculation crucially depend on the progress of these activities. These findings are consistent with those discussed in Fan et al. [7].

References

[1] Bolin, B., and C. D. Keeling, Large-scale atmospheric mixing as deduced from the seasonal and meridional variations of carbon dioxide, *J. Geophys. Res.*, *68*, 3899–3920, 1963.

[2] Conway, T., P. Tans, L. Waterman, K. Thonning, K. Masaire, and R. Gammon, Atmospheric carbon dioxide measurements in the remote global troposphere, 1981-1984, *Tellus*, *40B*, 81–115, 1988.

[3] Denning, A. S., et al., Three-dimensional transport and concentration of SF_6: A model intercomparison study (Transcom 2), *Tellus* (in press), 1999.

[4] Denning, A. S., I. Y. Fung, and D. Randall, Latitudinal gradient of CO_2 due to seasonal exchange with biota, *Nature*, *376*, 240–243, 1995.

[5] Enting, I. G., C. M. Trudinger, and R. J. F. H. Granek, Synthesis inversion of atmospheric CO_2 using the GISS tracer transport model, Technical Paper No. 29, CSIRO, Australia, 1993.

[6] Enting, I. G., C. M. Trudinger, and R. J. Francey, A synthesis inversion of the concentration and $\delta^{13}C$ of atmospheric CO_2, *Tellus*, *47B*, 35–52, 1995.

[7] Fan, S., M. Gloor, J. Mahlman, S. Pacala, J. Sarmient, T. Takahashi, and P. Tans, A large terrestrial carbon sink in north america implied by atmospheric and oceanic carbon dioxide data and models, *Science*, *282*, 442–446, 1998.

[8] Fung, I. Y., C. J. Tucker, and K. C. Prentice, Application of AVHRR vegetation index to study atmosphere-biosphere exchane of CO_2, *J.Geophys.Res.*, *92*, 2999–3016, 1987.

[9] Haas-Laursen, D. E., D. E. Hartley, and T.J. Conway, Consistent sampling methods for comparing models to CO_2 flask data, *J.Geophys.Res.*, *102*, 19059–19071, 1997.

[10] Keeling, C. D., M. Heimann, and S. C. Piper, A three dimensional model of atmospheric CO_2 transport based on observed winds: 4. Mean annual gradients and interannual variations, in *Aspects of Climate Variability in the Pacific and the Western Americas*, edited by D. H. Peterson, 305–363, AGU, Washington, 1989.

[11] Marland, G., T. A. Boden, R. C. Griffin, S. F. Huang, P. Kanciruk, and T. R. Nelson, Estimates of CO_2 emissions from fossil fuel burning and and cement manufacturing , based on the U.S.Bureau of Mines cement manufacturing data, ORNL/CDIAC-25 NDP-030, Carbn Dioxide Information Analysis Center, Oak Ridge National Laboratory, 1995.

[12] Masarie, K. A., and P. P. Tans, Extension and integration of atmospheric carbon dioxide data into a globally consistent measurement record, *J.Geophys.Res.*, *100*, 11,593–11,610, 1995.

[13] Nakazawa, T., K. Miyashita, S. Aoki, and M. Tanaka, Temporal and spatial variations of upper tropospheric and lower stratospheric carbon dioxide, *Tellus*, *43B*, 106–117, 1991.

[14] Pak, B. C., R. L. Langenfelds, R. J. Steele, and I. Simmonds, A climatology of trace gases from the Cape Grim overflights, 1992-1995, in *Baseline 94-95*, edited by R. J. Francey, A. L. Dick, and N. Derek, 41–52, Commonwealth of Australia, 1996.

[15] Pearman, G. I., and D. J. Beardsmore, Atmospheric carbon dioxide measurements in the Australian region: ten years of aircraft data, *Tellus*, *36B*, 1–24, 1984.

[16] Pearman, G. I., and P. Hyson, Activities of the global biosphere as reflected in atmospheric CO_2 records, *J. Geophys. Res.*, *85*, 4468–4474, 1980.

[17] Press, W. H., S. A. Teukolsky, W. T. Vetterling, and B. Flannery, *Numerical Recipes in Fortran, 2nd ed.*, Cambridge Univ. Press, New York, 1992.

[18] Rayner, P. J., and R. M. Law, A comparison of modeled responses to prescribed CO_2 sources, Technical Paper No. 36, CSIRO, Australia, 1995.

[19] Sellers, P., et al., Remote sensing of the land surface for studies of global change: Models - algorithms - expriments, *Remote Sens. Environ.*, *51(1)*, 3–26, 1995.

[20] Taguchi, S., A three-dimensional model of atmospheric CO_2 transport based on analyzed winds: Model description and simulation results for TRANSCOM, *J. Geophys. Res.*, *101*, 15099–15109, 1996.

[21] Tanaka, M., T. Nakazawa, and S. Aoki, Time and space variations of tropospheric carbon dioxide over japan, *Tellus*, *39B*, 3–12, 1987.

[22] WMO, WMO WDCGG data catalogue, GAW Data, Volume IV 13-Greenhouse gases and other atmospheric gases, World Meteorological Organization, Tokyo, Japan, 1997.

Figure 1: Annual mean flux of CO_2 over thirteen land areas and twelve oceanic area. Circles indicate the zero point for the relevant area and horizontal bar denotes the solution. Verticl arrows indicate the uncertainties of the solution derived from the covariance matrix. Ths size of flux is shown at the left bottom corner.

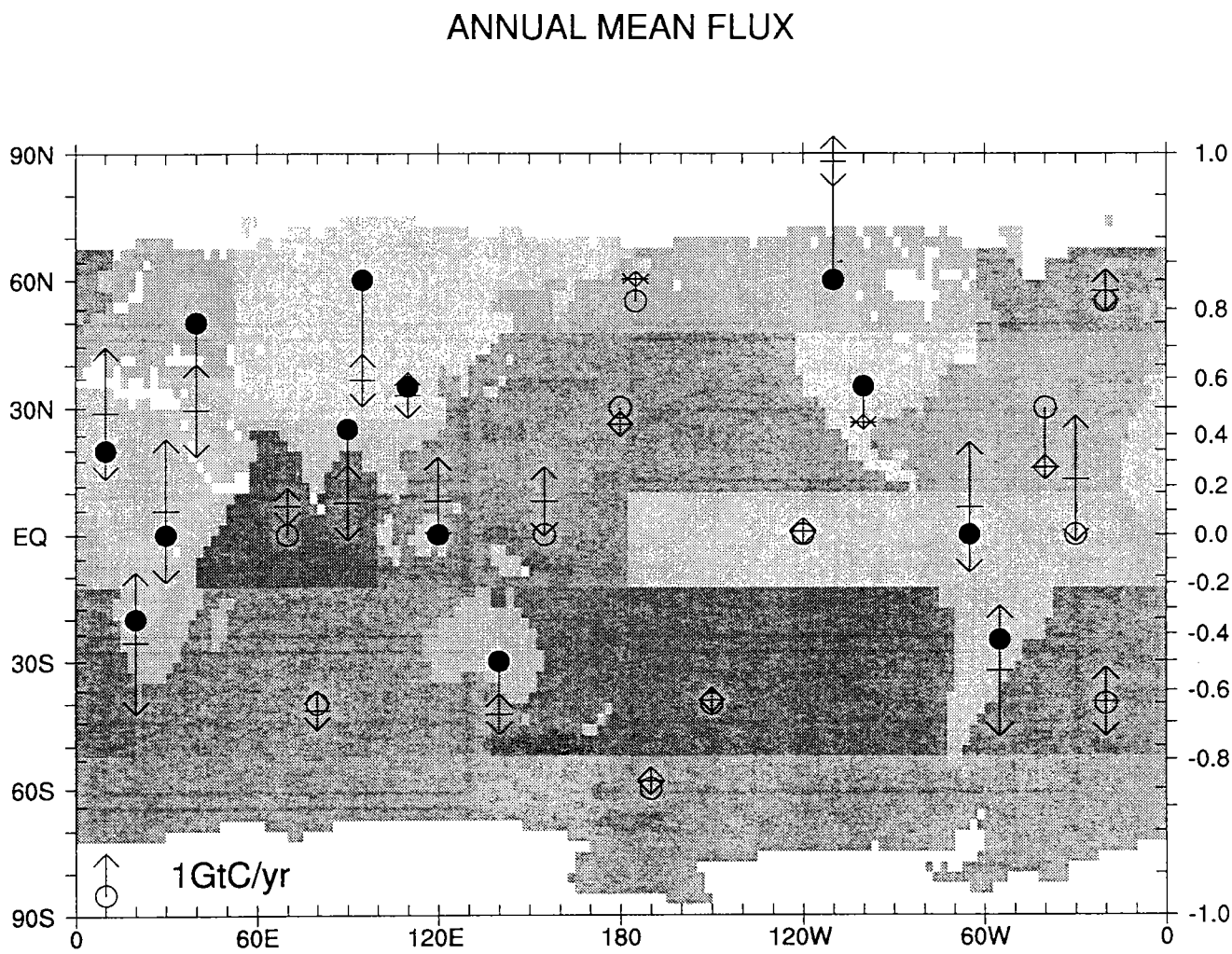

Figure 2: Seasonal cycle of CO_2 flux over thirteen land area. Dashed lines are for the estimates by *Fung et al.* [8].